Theoretical and experimental analysis of the near-edge x-ray absorption structure in MnTe and $Cd_{1-x}Mn_xTe$ alloys

J. Oleszkiewicz, M. Podgórny, and A. Kisiel
Instytut Fizyki, Uniwersytet Jagielloński, Krakow, Poland

E. Burattini
INFN, Laboratori Nazionali di Frascati, Frascati, Italy

(Received 6 October 1997; revised manuscript received 24 April 1998)

The x-ray absorption near edge structure (XANES) for $Cd_{1-x}Mn_xTe$ and MnTe in the hexagonal and zinc-blende structure has been studied and compared with the results of a self-consistent linear muffin-tin orbital calculation. It has been shown that *p-d* hybridization effects are strong enough to make XANES spectra at Te L_1 and L_3 edges sensitive to the energy position of the unoccupied Mn $3d\downarrow$ states. We present a unique method of finding the energy position of Mn $3d\downarrow$ states from analysis data from experiment and theoretical calculations. [S0163-1829(99)02631-4]

I. INTRODUCTION

Interest in the study of occupied and especially unoccupied electronic states in solids is steadily growing. Many efforts have been made to develop or modernize many different research and theoretical methods for that purpose.[1–6] The x-ray absorption spectroscopy (XAS), usually divided into x-ray absorption near-edge spectroscopy (XANES) and extended near-edge spectroscopy[7–9] (EXAFS) is recently employed. The XANES can be applied with success to the analysis of the conduction-band (CB) density of states (DOS) due to the several favorable features of this method when used in connection with synchrotron radiation facilities.[7] These features include very high accuracy of measurements, high sensitivity, very short acquisition time, and in general no limitations of the studied energy range. In addition, this technique is selective to atomic species and to the one component of the density of states.[10,11] The energy dependence of the transition matrix element is weak in the energy range near the absorption edge and, as a result, the XANES structures almost directly reflect the shape of the partial density of states of the unoccupied bands projected on the studied atom. Recent studies have shown that XANES for metals,[11] binary,[12,13] and semiconduction compounds[14–17] can be satisfactorily used.

The proper theoretical description of the band structure of the ternary semimagnetic semiconductors requires the inclusion of spin effects of the half-filled Mn $3d$ shell. In the framework of the spin-polarized bands of the usual one-electron picture the Mn $3d$ states are represented by only two exchange-split bands. The lower bands are fully occupied and spin polarized (spin up). The other ones are virtual and empty (Mn $3d$ spin-down states). The exchange splitting energy of these levels is usually calculated to be 4 to 6 eV. The biggest value of exchange splitting, obtained from the $X\alpha$ method, equal to 6 eV, corresponds to the situation with the biggest magnetic moment localized on Mn $3d\uparrow$ bands equal to $5\mu_B$.[18] But we should also expect intra-atomic Mn-based excitations. These lead to the many-electron multiplet theory. In this theory we have one ground state, $^6S_1$, and several quartet ($S=3/2$) excited states of Mn $3d^5$ ions, i.e., ^4P, ^4D, ^4F, ^4G. In crystal field the ground state became $^6A_1$ and the lowest excitation energy to the first state (i.e., $^4T_1$) is equal to about 2.1 eV. The mean energy difference between the ground state and all quartet states corresponds to the exchange energy splitting in the one-electron picture.[18] The possibilities of intra-atomic excitations, band-band excitations, and their combination lead to difficulties in the interpretation of the experimental data. The ultraviolet photoemission spectroscopy (UPS) measurement yields in $Cd_{1-x}Mn_xTe$ alloys show the spectra with a relatively sharp peak having a half-width of about 1 eV placed about 3.4 eV below the valence-band maximum.[19,20] This peak is commonly assigned to the nonhybridizing *e*-symmetric component of the Mn $3d\uparrow$ states. The t_2-symmetric Mn $3d\uparrow$ state component was assumed to hybridize significantly with the valence anion *p*-type states in a wide energy range. In addition, the analysis of the difference spectra shows a shoulder near the top of the valence band and a broad satellite in the energy 5–9 eV below the valence-band maximum (VBM).[21–23] It is commonly assumed that it is a result of many-body iteraction.[21–24] The energy position of the unoccupied virtual Mn $3d\downarrow$ bands is much more questionable than the respective situation for the Mn $3d\uparrow$ states. The interpretation of the optical absorption and reflectivity places the center of Mn $3d\downarrow$ states between 2.9 and 4.5 eV (Refs. 25 and 26) above VBM. The results of the bremsstrahlung isochromat spectroscopy (BIS) experiments for $Cd_{1-x}Mn_xTe$ made by Franciosi and co-workers[24,27,28] showed an additional increase in the intensity of the BIS spectrum with increasing Mn concentration. This was interpreted as a contribution of the Mn $3d\downarrow$ states placed about 5 eV above VBM and the Mn exchange splitting was estimated to be about 8.5 eV. It is almost twice as large as expected from earlier theoretical predictions.[29,30] The limitations of the local-density approximation (LDA) formalism was bland for it and a spin-polarized $(3d\downarrow)^5(4s\downarrow)^1(4p\downarrow)^1$-like ground state for Mn in this material was suggested. The different interpretation was

proposed from the first XANES measurements carried out for the $Cd_{0.5}Mn_{0.5}Te$ alloy and for MnTe in hexagonal and zinc-blende structures.[16,17] In this paper a full set of theoretical analysis of these results has been presented and discussed to elucidate the problems connected with the Mn $3d\downarrow$ states.

II. XANES MEASUREMENTS

The x-ray absorption measurements have been carried out with the use of synchrotron radiation at the Adone Wiggler facility in Frascati[31] utilizing a Si(111) channel-cut crystal monochromator. The original samples were high-purity monocrystaline $Cd_{1-x}Mn_xTe$ ($x=0.0$, 0.21, 0.52, and 0.7) grown by the Bridgman method in the Institute of Physics of the Polish Academy of Sciences in Warsaw. The samples were powdered and deposited on polyacetate films as required for XANES measurements. The resulting instrumental Gaussian broadening has been estimated for about 0.7 eV for Te and Cd $L_{1,3}$ edges and for about 1.0 eV for a Mn K edge. The contribution of each edge to the absorption coefficient has been extracted by extrapolating the pre-edge spectrum to higher energies by a Victoreen fit and by subtracting the fitted curve from the remaining experimental spectrum.[32] The complete set of experimental data for $Cd_{1-x}Mn_xTe$ with $x=0.21$, 0.52, and 0.7 and also for $Zn_{1-x}Mn_xTe$ with $x=0.5$ has been presented in a previous paper,[33] where the data were compared with theoretical results obtained from the calculation of the ferromagnetic phases of these materials using the standard linear muffin-tin orbital (LMTO) method.[34,35] In general good agreement was found, except for the comparison of Te $L_{1,3}$ edges and Cd $L_{1,3}$ edges, where growing discrepancies with an increase of the Mn concentration was visible. The disagreement was especially large in the slope of the x-ray absorption edge around the inflection point of the Te $L_{1,3}$ edges. This paper attempts to clarify this situation. For that purpose we have made a calculation for the antiferromagnetic phases using a modified LMTO method (see later in the next section).

III. ELECTRONIC STRUCTURE CALCULATIONS

The spin-polarized bands and density of states have been obtained using the self-consistent, semirelativistic LMTO method.[34,35] The exchange-correlation local spin density approximation (LSDA) potential was used in the form proposed by Vosko, Wilk, and Nusair.[36] The antiferromagnetic order of the Mn $3d$ spins has been used in calculations. It caused the alloy environment in $Cd_{0.5}Mn_{0.5}Te$ to be simulated by ordered supercells, which enlarge twice the volume of the primitive cell.[30] This makes the calculations for the antiferromagnetic structure more complicated than for the ferromagnetic structure[33] but better describes the physical situation of the $Cd_{0.5}Mn_{0.5}Te$ system.[30] The openness of the zinc-blende structure was dealt with in a standard way by placing additional ''empty spheres'' into a unit cell.[34] The calculations were carried out using the experimental lattice constants.

Such calculations for real materials have the main difficulty in adequate approximation of the self-energy operator even for very simple systems like Si, Ge, and LiCl.[42,43] The LSDA results do not produce discontinuity in a functional derivative of the exchange-correlation energy between valence and conduction bands, which is present in the many-body theory.[37–43] The LSDA calculations underestimate quasiparticles excitation energies and thus respective conduction-bands positions are too low, valence bands are too high, and the energy gap is too narrow. The results obtained from the many-body theory showed that the error in the energy position of the LSDA states is dependent on the nature of these states. The LSDA calculations give the wrong position of the unoccupied Mn $3d\downarrow$ bands in relation to the sp conduction bands in $Cd_{1-x}Mn_xTe$ alloys.[44] The unoccupied Mn $3d\downarrow$ states are placed at least 1–2 eV too low. The calculations place them in the energy gap, which does not agree with the experimental data.[29,30,45]

In order to find the true energy position of unoccupied Mn 3d states we modified the standard LMTO method. Our method could be divided into three steps. The first step was a normal self-consistent LMTO calculation. Next, we changed the potential parameter that defines the energy position of the weight point of the Mn $3d\downarrow$ states. The physical meanings of that parameter and the other potential parameters used in the LMTO method were discussed in detail by Skriver in his book.[35] The last step was the final calculation of the band structure and density of states with this modification. The increasing of the potential parameter caused the shifting of Mn $3d\downarrow$ states upwards and the rehybridization effects produced changes in the other states and their projected densities of states. We made several calculations with the Mn $3d\downarrow$ states energy position shifted by different values (0.0, 1.0, 2.0, and 4.0 eV). The results of such band-structure calculations formed a basis for x-ray absorption spectra calculations. The theoretical calculated spectra were compared with the experimental data.

IV. X-RAY ABSORPTION SPECTRA CALCULATIONS

According to the simple atomic-based selection rules, the edge L_1 is due to the electronic dipole transitions from the $2s$ core level to p-like conduction states and the $L_{2,3}$ edges are due to transitions from the $2p$ core level to s-like and d-like conduction states. The probabilities of the electronic quadruple transitions ($\Delta l=0,\pm 2$) for the Te and Cd $L_{1,3}$ edges are negligible.[11] The constant-matrix element approximation has been used, so the absorption spectra were obtained from relevant one-projected density of conduction states convoluted with Gaussian and Lorentzian functions. The Gaussian function reflects the instrumental resolution and the Lorentzian function reflects the core-level and final-state lifetime.[11,47] The calculations took into account the fact that the final-state lifetime is energy dependent. The part of the value of the Lorentzian width Γ_L that reflects the core-level lifetime was optimized to obtain the best agreement of the theoretical spectra with the experimental ones in the surrounding of the absorption edge (about 8 eV around the edge-first inflection point). In the LMTO calculation the number of bands calculated above the Fermi energy level is limited by the size of the basis function set. In addition, it is known that the LMTO method has second-order error in the $E-V_{VTZ}$, where V_{VTZ} is the average interstitial potential. Thence we do not expect a good description of conduction

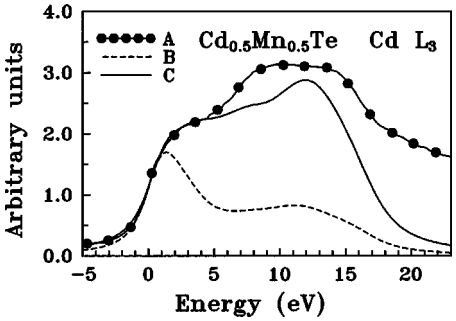

FIG. 1. Calculated Cd L_3 edge for $Cd_{0.5}Mn_{0.5}Te$. *A*, experimental spectrum; *B*, theoretical spectrum for the transition matrix element ratio $s:d=1:1$; *C*, theoretical spectrum for the optimized ratio $s:d\approx 1:3$.

states positioned higher than 1–2 Ry above V_{VTZ}. For this reason we modified the procedure of experimental data reduction presented in original form earlier.[13] In the procedure a limited energy range of the theoretical conduction density of states (DOS) for the x-ray absorption coefficient calculations was used. The energy was set to range from the conduction-band minimum (CBM) up to the energy cutoff fixed by us at about 17 eV. The original experimental spectra were modified by subtracting the part, which represents the absorption of hypothetical free-electron states above the energy cutoff.[13] According to Parratt,[46] that part is represented by the arctangent form. The energy position of the hypothetical free-electron part in relation to the original data inflection point was found from the alignment of the energy scale of experimental and theoretical spectra. An *ab initio* alignment of the theoretical and experimental energy scales is not possible because the LSDA calculations give a wrong value of the energy gap and do not give information on the chemical shifts. In addition, the inflection point of the absorption spectrum does not coincide with the conduction-band minimum. To align the energy scale, we shifted the experimental energy scale by a value that was optimized to obtain the best agreement of theoretical and experimental spectra in the vicinity of the absorption edge. The last fitting parameter was the *y*-scale normalization factor for the theoretical results. The standard computer nonlinear MINUIT minimalization procedure was used to calculate all fitted parameters.

As already mentioned above, the $L_{2,3}$ edges arise from the superposition of the transitions to *s*-like and *d*-like conduction states. The constant matrix element approximation causes an additional problem of the value of the ratio of the matrix elements of *s*- and *d*-like states. Assuming this ratio to be $s:d=1:1$ we obtained a very poor description for the Cd L_3 edge in $Cd_{0.5}Mn_{0.5}Te$. Thence optimization of the ratio was performed and the results are presented in Fig. 1. We found that the best agreement theory with experiment was for the ratio $s:d\approx 1:3$. The absorption coefficient is proportional to the square of the transition matrix element, so the *d*-like states have about 10 times bigger weight than *s*-like states. This result has been confirmed by the calculations with the inclusion of the dipole transition matrix elements that were done by Markowski, Oleszkiewicz, and Kisiel,[48] for pure CdTe.

V. THE RESULTS

A. CdMnTe

Figure 2 presents a projected density of conduction bands calculated for $Cd_{0.5}Mn_{0.5}Te$ with antiferromagnetic spin order. The figures present the results of calculations for normal

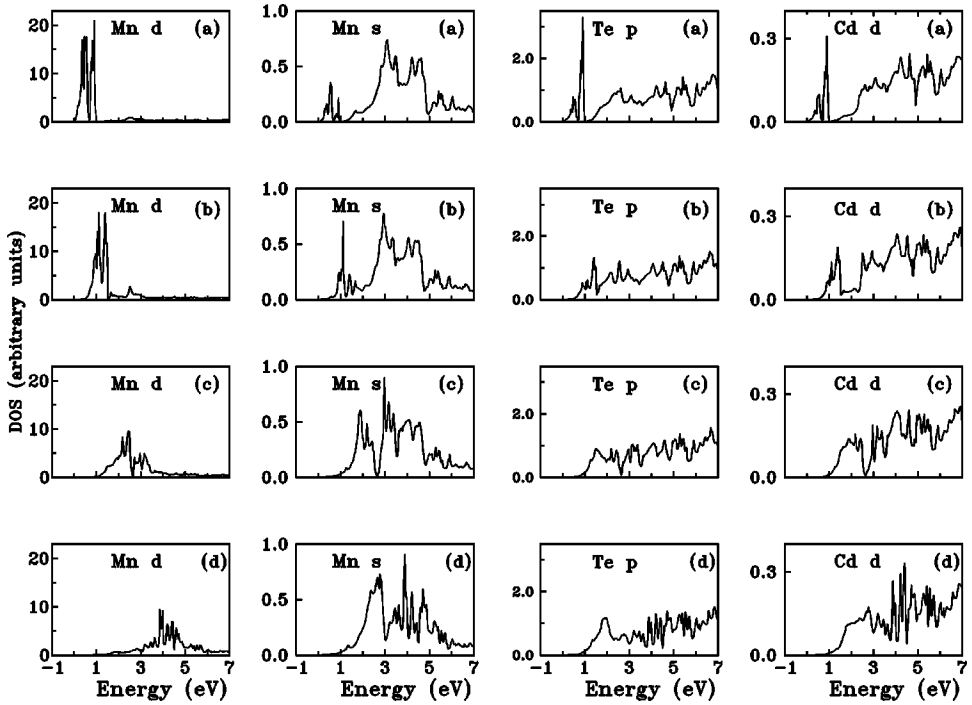

FIG. 2. Projected density of $Cd_{0.5}Mn_{0.5}Te$ conduction-band states per eV and cell for four theoretical cases of LSDA LMTO calculations. The theoretical calculation was done with potential parameters changed in such a way that the Mn $3d\downarrow$ states were shifted upwards by (a) 0 eV, (b) 1 eV, (c) 2 eV, (d) 4 eV. The zero of the energy scale was assigned to the top of valence bands.

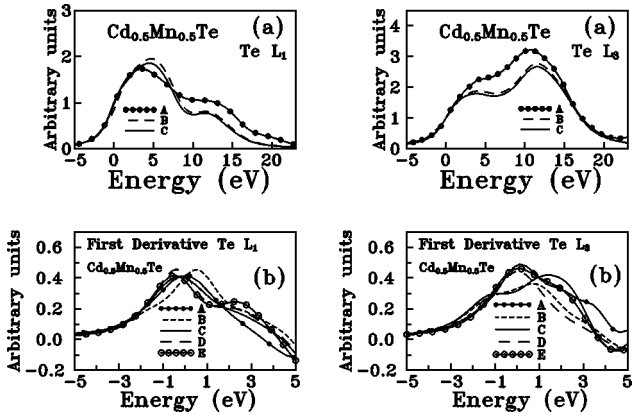

FIG. 3. Comparison of the experimental x-ray (curve *A*) $Cd_{0.5}Mn_{0.5}Te$ Te $L_{1,3}$ absorption spectra (a) and their derivatives (b) with the theoretical LSDA LMTO calculations, with the Mn $3d\downarrow$ states shifted upwards by 0 eV (*B*), 1 eV (*C*), 2 eV (*D*), and 4 eV (*E*). The zero of the energy axis was shifted to the first inflection point of the experimental spectrum.

self-consistent LSDA LMTO calculations [case (a)] and for calculation in which the average energy position of the Mn $3d\downarrow$ was shifted up in the energy scale by 1, 2, and 4 eV [cases (b), (c), and (d), respectively]. The result for case (a) compares very well with the result of Podgorny[30] or Wei and Zunger.[29] It is clearly seen that hybridization of the Mn $3d\downarrow$ states with other states is strong enough to cause a significant modification in the other component of projected DOS. These modifications are spread in the energy range with a width larger (more or less, depending on the case) than the width of the $3d\downarrow$. The LSDA calculations do not produce the true value for the energy gap, so to align the energy scale and to make comparison we shifted the energy scale in such way that for the case (a) the zero of the energy scale was placed at the bottom of the conduction bands. For the cases (b), (c), and (d) the energy scales were shifted in such way that the details of the DOS in the energy range very high above the conduction-bands minimum, where the influence of the Mn $3d\downarrow$ states is negligible, are the same for all cases. The calculated energy gap was equal to 1.3 eV for case (a),[30] as compared to 2.3 eV obtained from experiment.[45,49–51]

Figure 3(a) presents theoretical Te $L_{1,3}$ x-ray absorption spectra calculated from the normal LSDA LMTO results and from the LSDA LMTO calculations with a shifted energy position of the Mn $3d\downarrow$ states and their comparison to the experimental data. Neglecting the normalization the differences between two theoretical cases of the Te L_1 are very small. Therefore, even a significant modification of the DOS caused by rehybridization effects are almost disappearing as a result of convolution of the DOS with Lorentzian and Gaussian functions. In addition, the theoretical calculation based on the LMTO method used the basic functions set, which is limited and does not give a good description of the conduction bands lying far from the conduction-band minimum (CBM). We must concentrate the analysis in the area around the CBM, where the theoretical results are the most reliable. Thence (from about 5 eV below the CBM up to 5 eV above CBM) line shapes of calculated x-ray absorption edges show a weak dependence on the positions of the Mn $3d\downarrow$ states. Figure 3 serves as an example; it presents the

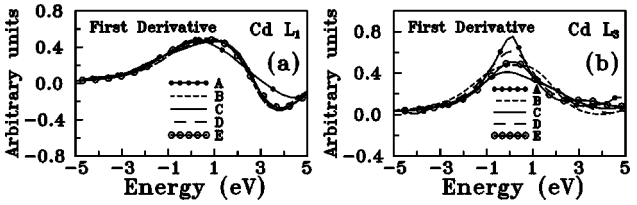

FIG. 4. First derivative of Cd $L_{1,3}$ x-ray absorption spectra near the absorption edge. The zero of the energy axis was shifted to the first inflection point of the experimental absorption spectrum (curve *A*). The theoretical calculation was done with potential parameters changed in such a way that the Mn $3d\downarrow$ states were shifted upwards by 0 eV (*B*), 1 eV (*C*), 2 eV (*D*), and 4 eV (*E*). The zero of the energy scale was assigned to the top of valence bands.

calculated line shape for Mn $3d\downarrow$ states unshifted (curve *A*) and shifted by 2 eV (curve *C*). But calculation of the first derivatives of the spectra [Fig. 3(b)] shows that the rehybridization effects are strong enough to produce significant modifications. We focus on the analysis of these modifications. The presented spectra for the Te L_1 and L_3 give the best agreement for a different position of the Mn $3d\downarrow$ states. We account for it by using in the calculations only the constant transition matrix approximation. The modifications of Te edges are bigger than modification of Cd edges (see Fig. 4), as we should expect, because the first-neighbor shell of the Mn ions in $Cd_{1-x}Mn_xTe$ is created by Te ions and only the second-neighbor shell of the Mn ions is created by Cd ions. We obtained the best common agreement between theoretical and experimental spectra in the case of calculations where the energy position of the center of the Mn $3d\downarrow$ states is shifted up by about 2 eV. The shifting of these states also causes a shift of the conduction-band minimum (CBM) by about 0.6 eV. This increased the calculated energy gap up to about 1.9 eV, being in a relatively good agreement with the experimental value equal to 2.3 eV.[45] Concluding all the above, we find that the center of the unoccupied Mn $3d\downarrow$ states is placed about 3.8 eV beyond the valence-band minimum. The shifting of the Mn $3d\downarrow$ states causes these states to become more energy delocalized—the energy width increased from 1 eV [case (a) in Fig. 2] up to 2.5 eV [case (c) in Fig. 2]. In addition, the value of the main peak of the Mn $3d\downarrow$ DOS was decreased by a factor of 2. It means that these states interact now much stronger with other conduction states than in the initial noncorrected LSDA results [case (a) in Fig. 2].

B. Hypothetical cubic MnTe

Many physical properties of $Cd_{1-x}Mn_xTe$ are almost linear with the Mn concentration. The limiting $x=1$ concentration is cubic MnTe.[45] Unfortunately, MnTe exists only in a NiAs structure, and the limiting concentration must be connected to a hypothetical MnTe with zinc-blende structure. The energy-gap behavior of the $Cd_{1-x}Mn_xTe$ versus Mn composition predicts the energy gap for zinc-blende MnTe to be about 3.2 eV. The present theoretical calculations show the energy gap to be about 0.8–1.0 eV.[29,30,44] This disagreement is caused by placing the unoccupied Mn $3d\downarrow$ states too low. We calculated several times the electronic band structure of the zinc-blende antiferromagnetic MnTe by the modi-

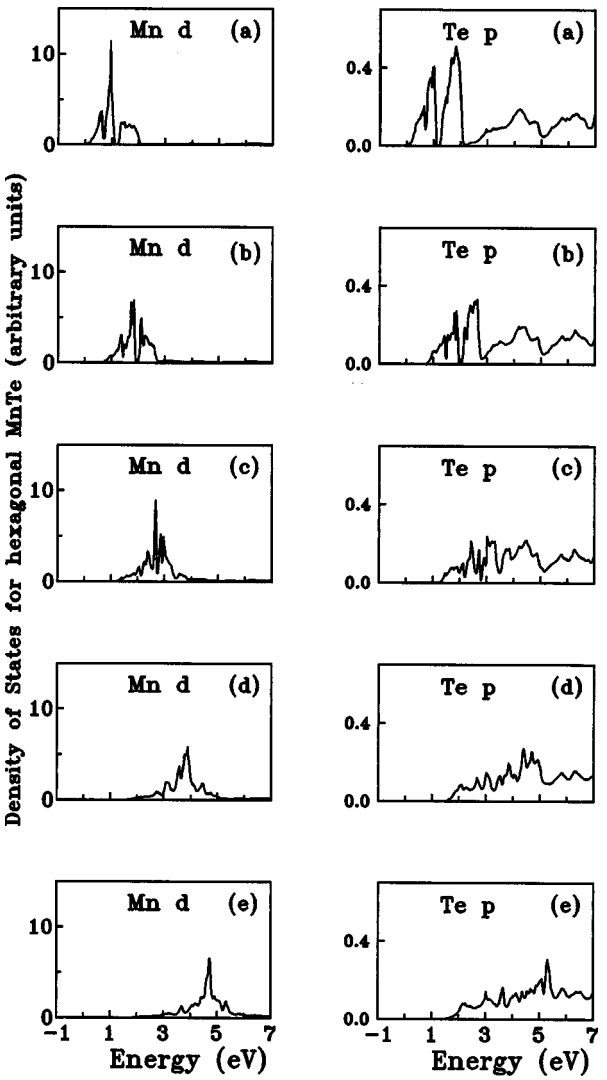

FIG. 5. Projected density of hypothetical zinc-blende structure MnTe conduction-band states per eV and cell for five theoretical cases of LSDA LMTO calculations. The theoretical calculation was done with potential parameters changed in such a way that the Mn $3d\downarrow$ states were shifted upwards by (a) 0 eV, (b) 1 eV, (c) 2 eV, (d) 4 eV. The zero of the energy scale was assigned to the top of valence bands.

fied LMTO method by arbitrarily shifting the center of the unoccupied Mn $3d\downarrow$ states. The DOS results are presented in Fig. 5. To compare the theory with experiment we need the experimental results of their hypothetical zinc-blende MnTe. This result was *extracted* from an experimental $Cd_{1-x}Mn_xTe$ data set in a way ''similar'' to the idea of virtual crystal approximation (VCA) for x-ray spectra:[33]

$$Cd_{1-x}Mn_xTe=(1-x)CdTe+xMnTe. \tag{5.1}$$

Figure 6 presents a comparison of the extracted data with theoretical calculated x-ray absorption spectra. Clearly, the uncorrected LSDA result does not agree with the experiment. The calculated x-ray absorption spectrum for Te L_1 has two peaks while the experimental spectrum has only one peak. The shape of the calculated Te L_1 spectrum is drastically changed by a shift of the center of $3d\downarrow$ states. The best agreement of theory and experiment was obtained for the Te

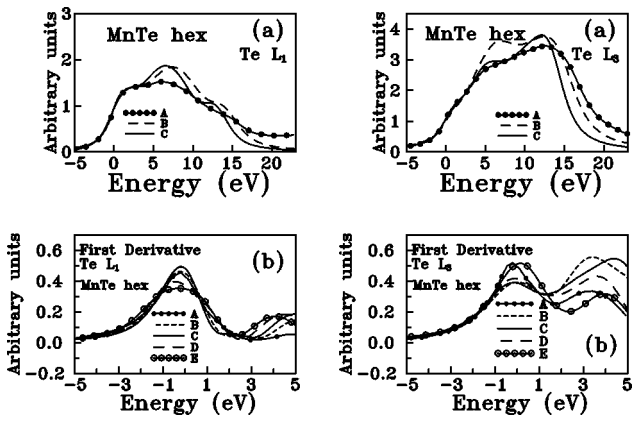

FIG. 6. Comparison of the experimental (curves *A*) Te $L_{1,3}$ absorption spectra (a) and their derivatives with theoretical LSDA LMTO calculations for the hypothetical zinc-blende structure MnTe. The theoretical LMTO calculations were done to shift the Mn $3d\downarrow$ states upwards by 0 eV (*B*), 1 eV (*C*), 2 eV (*D*), and 3 eV (*E*). The zero of the energy axis was shifted to the first inflection point of the experimental spectrum.

$L_{1,3}$ edges after shifting the center of the Mn $3d\downarrow$ states by about 3 eV up. The change of the energy position of these states causes the change of the interaction of the $3d\downarrow$ states with the others. The interactions are now stronger than before, but this effect seems to be weaker than for $Cd_{0.5}Mn_{0.5}Te$ because the energy width of the $3d\downarrow$ states was increased from 1.7 eV up to only 2 eV. The center of the Mn $3d\downarrow$ states has been placed at about 4 eV above the VBM. The process of shifting the center of the $3d\downarrow$ states caused the shift up of the CBM and increased the energy gap up to 2.8–3.0 eV.

C. Hexagonal MnTe

The study of the Te $L_{1,3}$ edges for hexagonal MnTe was completed by the same method as for $Cd_{0.5}Mn_{0.5}Te$. Figures 7 and 8 show the results. The calculated shape of the x-ray absorption spectra differs from the experimental ones much more than for $Cd_{0.5}Mn_{0.5}Te$ and zinc-blende MnTe. The shifting of the Mn $3d\downarrow$ states does not produce a significant change in the shape but only very weak changes of edges (about 4 eV around the first inflection point) visible only on making the first derivatives of the spectra. The Te L_1 spectra in the area around the first inflection point are almost insensitive to the shifting of these states up to 2 eV. The Te L_3 edge is more sensitive than the Te L_1 edge and the best agreement of theory with experiment was obtained for a 3-eV shift, but for this shift the agreement for Te L_1 becomes worse for smaller shifts. The shift of 2.5 eV seems to be a good compromise for both edges. As a consequence the center of the Mn $3d\downarrow$ states is placed about 3.75 eV above the VBM.

VI. DISCUSSION

From the presented results it follows that LSDA LMTO calculations produce x-ray absorption edge spectra which do not fit very well with experimental ones, while the same LSDA LMTO calculation, corrected by a shift in the energy position of the Mn $3d\downarrow$ states, improves the agreement sig-

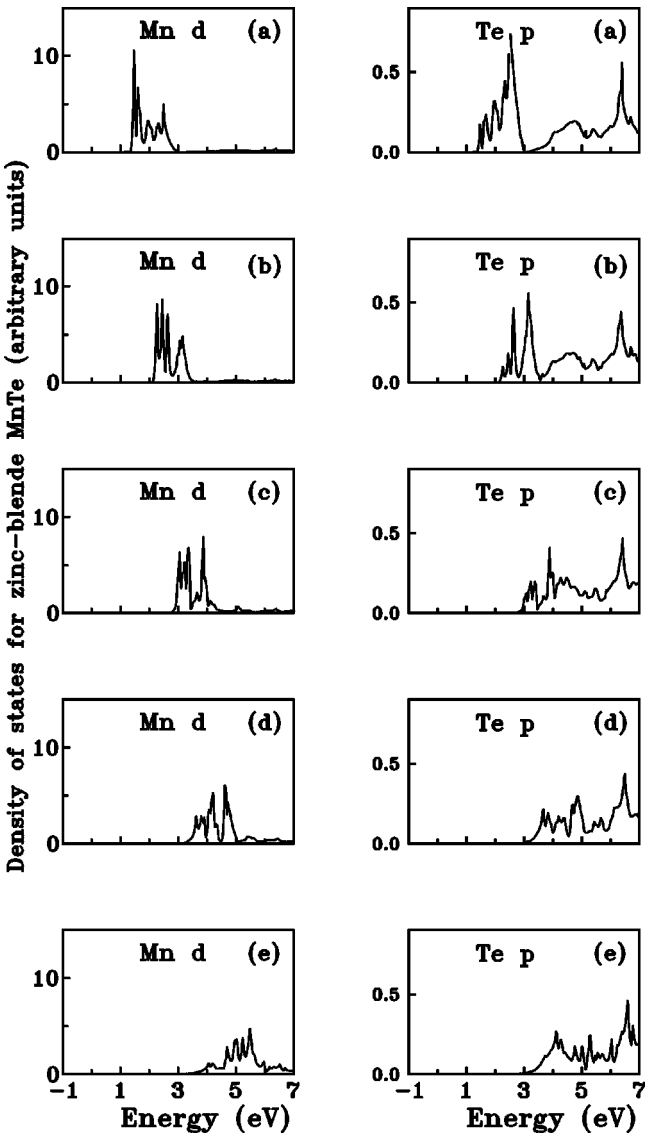

FIG. 7. Projected density of the hexagonal MnTe conduction-band states per eV and cell for five theoretical cases of LSDA LMTO calculations. The theoretical calculations were done with potential parameters changed to shift the Mn $3d\downarrow$ states upwards by (a) 0 eV, (b) 1 eV, (c) 2 eV, (d) 4 eV. The zero of the energy scale was assigned to the top of the valence bands.

nificantly. The energy position of the Mn $3d\downarrow$ states has significant influence on the Te $L_{1,3}$ edges and, in a weaker way, on the Cd $L_{1,3}$ edge. The transitions that produce Te $L_{1,3}$ edges are localized on a Te site and cause big changes in

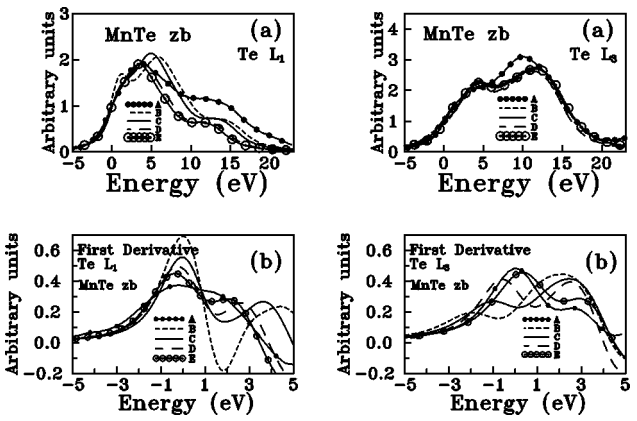

FIG. 8. Comparison of the experimental (curves *A*) Te $L_{1,3}$ absorption spectra (a) and their derivatives with theoretical LSDA LMTO calculations for hexagonal MnTe. The theoretical LMTO calculations were done to shift the Mn $3d\downarrow$ states upwards by 0 eV (*B*), 1 eV (*C*), 2 eV (*D*), and 3 eV (*E*). The zero of the energy axis was shifted to the first inflection point of the experimental spectrum.

the occupancy of the states localized on the Te site and negligible changes of the occupancy of the states localized on the Mn site. It means that the correlation and relaxation effects connected with the Mn $3d\downarrow$ states are relatively negligible in the transitions which produce Te $L_{1,3}$ edges. The conclusion, which we draw from the above, is that the method presented in this paper allows us to determine the energy position of the Mn $3d\downarrow$ states with good accuracy (Table I). The shift of the energy position of the Mn $3d\downarrow$ states increases the energy gap. It is surprising that the theoretical x-ray absorption spectra, which best fit the experimental ones, have been obtained from the calculations giving also the best agreement of the energy gap with experimental values (Table I).

Table I also presents the value for the exchange splitting of the Mn $3d$ states. These values have been obtained using the described method and from the experimental values of the energy gap and the energy position of the occupied Mn $3d\uparrow$ states. It is rather surprising that these values are so big; in fact, they are much bigger than the values predicted by earlier theoretical works. Our value of the exchange splitting is a little smaller than the value of 8.3 ± 0.4 obtained by Franciosi *et al.*[27,24] It was thus suggested that a big exchange splitting is caused by an artificial configuration with total spin-polarized Mn $(3d\uparrow)^5$ states and with additional spin-polarized Mn $(s\uparrow)^1$ and Mn $(p\uparrow)^1$ states. We agree that the local density-functional theory has many limitations when

TABLE I. Energy position of the Mn $3d\downarrow$ states above CBM, E($3d\downarrow$), value of the exchange splitting of the Mn $3d$ states, ΔE_X, and the energy gap E_g from our method. The results are in eV.

	$E\ (3d\downarrow)$	ΔE_X	E_g	
			theory	experiment
$Cd_{0.5}Mn_{0.5}Te$	1.75 ± 0.25	7.60 ± 0.35	1.90 ± 0.2	2.30 ± 0.02 [a]
hexagonal MnTe	2.20 ± 0.25	7.25 ± 0.35	1.20 ± 0.2	1.27 ± 0.02 [b]
zinc-blende MnTe	1.50 ± 0.25	7.50 ± 0.35	2.90 ± 0.2	3.20 ± 0.1 [a]

[a]See Refs. 45 and 49–51.

[b]See Refs. 50 and 51.

TABLE II. Results of fitting of the Γ_L core-level width.

	Te L_1	Te L_3	Cd L_1	Cd L_3
$Cd_{0.5}Mn_{0.5}Te$	2.25±0.1	2.1±0.1	2.00±0.1	2.40±0.1
hexagonal MnTe	2.10±0.2	2.4±0.2		
zinc-blende MnTe	2.40±0.2	2.4±0.2		

describing systems like $Cd_{1-x}Mn_xTe$. The LSDA approximation generally gives bad descriptions of the excitations energies, as we discussed in Sec. III. We hope that the calculations that include the self-energy operator, or at least LSDA calculations with corrections arising from the self-energy operator, describe all the electronic states in semimagnetic semiconductor compounds much better.

The method presented in this paper also gives additional results. Table II presents the value of the core-level width Γ_L, and Table III contains the energy position of the first inflection point of the edges in relation to the conduction-band minimum. These results depend on the details of the calculation (i.e., the energy position of the Mn $3d\downarrow$ states). In Table III the results corresponding to the best agreement of the theoretical and experimental x-ray absorption spectra are presented. The error of the Γ_L width has been taken from the fitting. The error of the energy position of the Mn $3d\downarrow$ is not easy to be estimated. It is observed that the study of the Te L_3 edge gives a value of the energy localization of the center of the Mn $3d\downarrow$ states a little bigger than the value obtained from the study of the Te L_1 edge. It is the case for all three studied compounds, i.e., $Cd_{0.5}Mn_{0.5}Te$, zinc-blende MnTe, and hexagonal MnTe. The observed discrepancy can be explained as a result of using a constant transition matrix approximation. The different energy dependence of the transition matrix element from the core state to s,p,d-like conduction states can be an explanation of the facts mentioned above. A significant role can also be played by some relaxation and correlation effects, which are usually stronger for states with a greater l number. The fitting procedure was focused in the 10-eV energy range around the inflection point of the edges. The accuracy of the energy position of the Mn $3d\downarrow$ is estimated after an analysis of all the edges. The energy gap is connected with the energy position of the center of Mn $3d\downarrow$. The value of the energy gap changes significantly by only a small shift of the center of the Mn $3d\downarrow$—in the range 0–2 eV. For a larger shift the energy gap almost does not change. As a result the accuracy of the energy gap is better than the accuracy of the energy position of the Mn $3d\downarrow$ states.

TABLE III. Position of the edge-first inflection point in relation to the conduction-band minimum: $\Delta E = E_0 - E_{CBM}$. The quantities are in eV.

	Te L_1	Te L_3	Cd L_1	Cd L_3
$Cd_{0.5}Mn_{0.5}Te$	1.6±0.1	1.50±0.10	2.05±0.05	0.70±0.05
hexagonal MnTe	1.5±0.2	0.68±0.14		
zinc-blende MnTe	1.6±0.1	1.48±0.08		

VII. CONCLUSION

We presented a method that allows us to localize the energy position of the unoccupied Mn $3d\downarrow$ states. The method is based on the study of the details of the Te $L_{1,3}$ x-ray absorption edges. The transitions, which produce Te $L_{1,3}$ absorption lines, are localized on Te sites, so we should expect that the correlation and relaxation effects that arise during these transitions do not have significant influence on the energy position of the Mn $3d\downarrow$ states (localized on the Mn site). The mechanism is clearer than in the case of the optical transition from the valence to conduction states. For the optical transition the correlation and relaxation effects are very strong, which leads to difficulties in the interpretation of the experimental and theoretical results.[25,29,30] The presented procedure is a unique method to establish the energy position of the unoccupied Mn $3d\downarrow$ states in the $Cd_{1-x}Mn_xTe$-like systems. The energy accuracy of this method was estimated to be about 0.4± eV. To establish the energy position with better accuracy, a theory should be applied that does not have a constant transition matrix approximation but that does have a big function set describing precisely the electronic band structure in a very wide energy scale (at least 50 eV).

ACKNOWLEDGMENTS

We would like to thank A. Mycielski for supplying us with the $Cd_{1-x}Mn_xTe$ samples. This work was supported in part by the Polish Central Research program CPBP 01.12 and by the State Committee for Scientific Research (Grant No. PB-2528/2/91).

[1] A. Kisiel, M. Zimnal-Starnawska, E. Antonangeli, M. Piacentini, and N. Zema, Nuovo Cimento D **8**, 436 (1986).
[2] F. Bassani and G. Pastori-Paravicini, *Electronic States and Optical Transition in Solids* (Pergamon, Oxford, 1975).
[3] J. B. Pendry and J. F. L. Hopkinson, J. Phys. (Paris) **39**, 142 (1978).
[4] J. B. Pendry, J. Phys. C **14**, 1381 (1981).
[5] W. Speier, J. C. Fuggle, P. Durham, R. Zeller, R. J. Blake, and P. Stern, J. Phys. C **21**, 2621 (1988).
[6] D. D. Woodruff, N. V. Smith, P. D. Johnson, and W. A. Royer, Phys. Rev. B **26**, 2943 (1982).
[7] *Synchrotron Radiation*, edited by C. Kunz, *Topics in Current Physics* Vol. 10 (Springer, Berlin, 1979), p. 1.
[8] P. A. Lee, P. H. Citrin, P. Eisenberger, and B. M. Kincaid, Rev. Mod. Phys. **53**, 769 (1981).
[9] *EXAFS and Near Edge Structure III*, Proceedings of the International Conference, Stanford, 1984, edited by K. O. Hodgson, B. Hedman, and J. E. Penner-Hahn (Springer-Verlag, Berlin, 1984).
[10] J. E. Müller, O. Jepsen, and J. W. Wilkins, Solid State Commun. **42**, 365 (1982).
[11] J. E. Müller and J. W. Wilkins, Phys. Rev. B **29**, 4331 (1984).
[12] C. Sagiura and S. Muramatsu, Phys. Status Solidi B **129**, K157 (1985).

[13] A. Kisiel, G. Dalba, P. Fornasini, M. Podgorny, J. Oleszkiewicz, and E. Burattini, Phys. Rev. B **39**, 7895 (1989).
[14] A. Kisiel, A-I Ali Dahr, P. M. Lee, G. Dalba, P. Fornasini, F. Rocca, and E. Burattini, Proceedings of the 2nd European Conference on Progress in X-Ray Synchrotron Radiation Research, Bologna, 1990, edited by A. Balerna, E. Bernieri, and S. Mobilio (SIF, Bologna, 1990), p. 855.
[15] M. Podgórny, A. Kisiel, J. Oleszkiewicz, G. Dalba, P. Fornasini, and E. Burattini, Proceedings of the 2nd European Conference on Progress in X-Ray Synchrotron Radiation Research, Bologna, 1990 (Ref. 14), p. 859.
[16] J. Oleszkiewicz, M. Podgórny, A. Kisiel, G. Dalba, F. Rocca, and E. Burattini, Proceedings of the 2nd European Conference on Progress in X-Ray Synchrotron Radiation Research, Bologna, 1990 (Ref. 14), p. 863.
[17] A. Kisiel, J. Oleszkiewicz, and M. Podgórny, J. Cryst. Growth **101**, 237 (1990).
[18] J. C. Slater, *The Self-consistent Field for Molecules and Solids* (McGraw-Hill, New York, 1974).
[19] M. Taniguchi, L. Ley, R. C. Johnson, J. Ghijsen, and M. Cardona, Phys. Rev. B **33**, 1206 (1986).
[20] L. Ley, M. Taniguchi, J. Ghijsen, R. C. Johnson, and A. Fuijmori, Phys. Rev. B **35**, 2839 (1987).
[21] A. Fujimori and F. Minami, Phys. Rev. B **30**, 957 (1984).
[22] A. Fujimori, M. Sacki, N. Kimizuka, M. Taniguchi, and S. Suga, Phys. Rev. B **34**, 7318 (1986).
[23] M. Taniguchi, M. Fujimori, M. Fujisawa, T. Mori, I. Souma, and Y. Oka, Solid State Commun. **62**, 431 (1987).
[24] A. Franciosi, A. Wall, Y. Gao, J. H. Weaver, M. H. Tsai, J. D. Dow, R. V. Kasowski, R. Reifenberger, and F. Pool, Phys. Rev. B **40**, 12 009 (1989).
[25] A. Kisiel, M. Piacentini, F. Antonangeli, J. Oleszkiewicz, A. Rodzik, N. Zema, and A. Mycielski, J. Phys. C **20**, 5601 (1987).
[26] J. Oleszkiewicz, A. Kisiel, and A. Rodzik, Solid State Commun. **63**, 77 (1987).
[27] A. Franciosi, A. Wall, Y. Gao, J. H. Weaver, S. Chang and A. Raisanen, in *Proceedings of the 19th International Conference on the Physics of Semiconductors, Warsaw, 1988*, edited by W. Zawadzki (Institute of Physics, Polish Academy of Science, Wrocław, Poland, 1988), p. 1263.
[28] A. Wall, A. Franciosi, Y. Gao, J. H. Weaver, M. H. Tsai, J. D. Dow, and R. V. Kasowski, J. Vac. Sci. Technol. A **7**, 656 (1989).
[29] Su-Huai Wei and A. Zunger, Phys. Rev. B **35**, 2340 (1987).
[30] M. Podgórny, Z. Phys. B **69**, 501 (1988).
[31] E. Burattini, E. Bernieri, A. Balerna, C. Menuccini, R. Rinzivillo, G. Dalba, and P. Fornasini, Nucl. Instrum. Methods Phys. Res. A **246**, 125 (1986).
[32] B. T. Teo, *EXAFS: Basic Principles and Data Analysis* (Springer, Berlin, 1986).
[33] A. Kisiel, A-I Ali Dahr, P. M. Lee, P. Fornasini, and E. Burattini, Phys. Rev. B **44**, 11 075 (1991).
[34] O. K. Anderson, Phys. Rev. B **12**, 3060 (1975).
[35] H. L. Skriver, *The LMTO Method*, edited by M. Cardona, P. Fulde, and H. J. Queisser, Solid State Sciences, Vol. 41 (Springer, Berlin, 1984).
[36] S. H. Vosko, L. Wilk, and M. Nusair, Can. J. Phys. **58**, 1200 (1980).
[37] P. Hohenberg and W. Kohn, Phys. Rev. **136**, B864 (1964).
[38] W. Kohn and L. J. Sham, Phys. Rev. **140**, A1133 (1965).
[39] L. J. Sham and W. Kohn, Phys. Rev. **145**, 561 (1966).
[40] T. Koopmans, Physica (Amsterdam) **1**, 104 (1933).
[41] L. Hedin and S. Lundqvist, *Solid State Physics*, edited by H. Ehrenreich, D. Turnball, and F. Seitz (Academic, New York, 1969), Vol. 23, p. 1.
[42] M. S. Hybersten and S. G. Louie, Phys. Rev. B **34**, 5390 (1986).
[43] W. Linden and P. Horsch, Phys. Rev. B **37**, 8351 (1988).
[44] B. E. Larson, K. C. Hass, H. Ehrenreich, and A. E. Carlson, Phys. Rev. B **37**, 4137 (1988).
[45] O. Goede and W. Heimbrodt, Phys. Status Solidi B **146**, 11 (1988), and references within.
[46] L. G. Parrat, Rev. Mod. Phys. **31**, 616 (1959).
[47] P. Horsch, W. Linden, and W. D. Luckas, Solid State Commun. **62**, 359 (1987).
[48] R. Markowski, J. Oleszkiewicz, and A. Kisiel, Acta Phys. Pol. A **80**, 369 (1991).
[49] M. Zimnal-Starnawska, M. Podgórny, A. Kisiel, A. Giriat, M. Demianiuk, and J. Żmija, J. Phys. C **17**, 615 (1984).
[50] J. W. Allen, G. Lucovsky, and J. C. Mikkelson, Solid State Commun. **24**, 367 (1977).
[51] J. Oleszkiewicz, A. Kisiel, and S. A. Ignatowicz, Thin Solid Films **175**, 1 (1988).